# Solvation and reorganization energies in polarizable molecular and continuum solvents

Joel S. Bader, Christian M. Cortis, and B. J. Berne

Citation: The Journal of Chemical Physics **106**, 2372 (1997); doi: 10.1063/1.473790
View online: http://dx.doi.org/10.1063/1.473790
View Table of Contents: http://scitation.aip.org/content/aip/journal/jcp/106/6?ver=pdfcov
Published by the AIP Publishing

# Solvation and reorganization energies in polarizable molecular and continuum solvents

Joel S. Bader
*CuraGen Corporation, 322 East Main Street, Branford, Connecticut 06405*

Christian M. Cortis
*Department of Biochemistry and Molecular Biology, Columbia University, New York, New York 10027*

B. J. Berne
*Department of Chemistry, Columbia University, New York, New York 10027*

(Received 4 June 1996; accepted 30 October 1996)

The solvation free energy difference, $\Delta G$, and reorganization energy, $\lambda$, of the electronic transition between the ground and first excited state of formaldehyde are investigated as a function of the solvent electronic polarizability in aqueous solution. Solvent shifts are difficult to measure experimentally for formaldehyde due to oligomer formation; shifts for acetone, which have been measured experimentally, are used instead for comparison with computational results. Predictions of the Poisson–Boltzmann equation of dielectric continuum theory with molecular shaped cavities and charges on atomic sites calculated from *ab initio* quantum chemistry are compared with direct molecular dynamics simulations using the fluctuating charge model of polarizable water. The explicit molecule simulations agree with the acetone experimental results, but the continuum dielectric calculations do not agree with explicit solvent or with experiment when the default model cavity is used for both the ground and excited state molecule. Several different algorithms are used to define the size of the molecular cavity in the ground and excited states, but we are unable to find a single set of atomic radii that describe adequately all the data. Quantitative calculations from a continuum model might therefore require charge-dependent solute cavity radii. © *1997 American Institute of Physics.* [S0021-9606(97)50206-6]

## I. INTRODUCTION

Charge transfer underlies fundamental and important biological and physical processes ranging from photosynthesis to respiration. Much of our current theoretical understanding of charge transfer processes rests on Marcus theory, which describes how fluctuations in the solvent allow transitions between the electronic states of a solvated charge transfer system.[1–4] These solvent fluctuations are in turn based on a harmonic model for the electric polarization modes of the solvent. Advances in experimental and computational technology allow a closer examination of solvation, and a greater understanding of how the solvation energy arising from a collection of explicit molecules can generate solvation energies that appear harmonic and generally obey linear response.

The difference in the solvent response of classical orientational degrees of freedom and of quantal electronic degrees of freedom has prompted recent attention. For equilibrium properties, such as solvation free energies ($\Delta G$), the classical modes and the quantum modes provide full solvation. The total solvent response, represented by the static dielectric $\epsilon_0$, describes the solvation free energy for a solute at equilibrium.

Nonequilibrium properties, however, bring in a time scale that can modify the contribution of different modes. An extreme example of such a nonequilibrium property is the solvent shift in a condensed-phase absorption spectrum for a solute. The electronic polarization modes of the solvent have a quantum mechanical response that often is contained implicitly in the Born–Oppenheimer energy surfaces for the ground and excited state solute. These quantum mechanical modes provide full instantaneous response, which is represented by the optical dielectric constant $\epsilon_\infty$. The classical orientational degrees of freedom require time to equilibrate to the new solute state and are thus fixed during the electronic transition. The solvent reorganization required to achieve equilibrium around the changed solute electronic state is termed the reorganization energy ($\lambda$).

Before proceeding, we note that it is an approximation to assume that the orientational modes behave classically. Indeed, even a nonpolarizable solvent can require a quantum mechanical treatment for high-frequency nuclear modes like librations and vibrations. Quantum effects from nuclear modes have been studied in charge transfer using methods based on correlation functions that impose a harmonic form on the quantum fluctuations.[5–11] Path integral methods, which do not require a harmonic approximation, have been used more recently to study quantum effects in similar charge transfer reactions.[8,12–14] Although the quantization of the solvent nuclear modes can be treated accurately with a path integral representation, we do not include quantum nuclear effects to focus specifically on electronic polarizability.

Recently, there has been considerable discussion regarding the proper treatment of electronic and orientational polarization modes in charge transfer reactions.[15–18] Any model with solvent modes that respond linearly can be used to

 0021-9606/97/106(6)/2372/16/$10.00 

make specific predictions for the dependence of quantities such as $\Delta G$ and $\lambda$ on the solvent parameters $\epsilon_0$ and $\epsilon_\infty$. These arguments are often constructed in terms of idealized solutes consisting of a monopole or a dipole embedded in the center of a spherical cavity surrounded by a continuum fluid with a frequency-dependent dielectric.

We recently reported the results of such a study.[19] Computer simulations were performed for a model of the charge transfer during an electronic transition of formaldehyde in explicit water solvent. Different sets of simulations employed polarizable and nonpolarizable solvent molecules. The simulation results were compared with predictions of a dielectric continuum theory in which the solute was idealized as a spherical cavity with a central point dipole. The continuum solvent was assigned low frequency and high frequency dielectric constants $\epsilon_0$ and $\epsilon_\infty$ equal to the values for the bulk molecular solvent. With this simplified model and a single cavity size for both the ground and excited states, we could not obtain good agreement with $\Delta G$ and $\lambda$ obtained from simulation. Using different ground and excited state cavity sizes in the continuum calculation improved the agreement with explicit molecular simulations, but produced unrealistically narrow absorption and fluorescence spectra compared to simulation results.

In addition to providing a theoretical footing for describing solvation, dielectric continuum models based on the Poisson–Boltzmann equation are being used as practical and efficient routes to solvation energies and understanding how the condensed phase modifies molecular interactions and electronic structure.[20–24] Related methods use a lattice of polarizable point dipoles to mimic a dielectric.[25,26] These methods retain a molecular description of the solute and offer a faster but less detailed description of solvation, compared to fully atomistic simulations.

In this report, we investigate the importance of an atomistic treatment of the solute by comparing dielectric continuum calculations using a molecular solute with calculations for a spherical solute with a point dipole at its center. The dielectric continuum calculations are also compared with the results of fully atomiztic molecular dynamics simulations. The atomiztic solute mimics the excluded volume of formaldehyde by defining a spherical radius for each of the formaldehyde atoms. Embedded in this molecular-shaped cavity are point charges that depend on the solute electronic state.

In order to test the role of molecular polarizability, several different solvent models are used in the molecular simulations. One of the solvent models is the recently introduced polar, polarizable TIP4P-FQ (abbreviated FQ) model, which employs fluctuating charges for an efficient representation of polarizable water.[27] We also consider a series of nonpolarizable water models: TIP4P-FQ/MQ,[19] TIP4P-MQ,[19] and TIP4P.[28] The simulations provide essentially exact results for $\Delta G$ and $\lambda$ for the models we consider. The simulations can also be used to measure the role that solvent polarizability plays in determining $\Delta G$ and $\lambda$. These simulation results are compared with the results calculated using a molecular cavity and a continuum solvent. The comparison is significant because many simulations employ a nonpolarizable molecular solvent and then use predictions provided by dielectric continuum theory to correct for solvent polarizability.

The formaldehyde electronic transition used as the basis of this study is the $n \rightarrow \pi^*$ electronic transition from the $^1A_1$ ground state to the $^1A_2$ excited state. The solvent shift for a similar transition in the carbonyl carbon of acetone is known to be 1900 $cm^{-1}$, equivalent to 5.4 kcal/mol.[29] The shift for the formaldehyde line is less certain due to the formation of oligomers or ketals in aqueous solution. However, the shift for the gas phase transition for an isolated formaldehyde molecule is thought to be similar to the acetone shift.

The solvated formaldehyde $n \rightarrow \pi^*$ transition has also been studied extensively by theoretical methods: quantum-mechanical treatments,[30–39] simulations of formaldehyde in water clusters,[40] and simulations in bulk solvent.[19,40–42] (A summary of the findings of many of the studies can be found in Ref. 39.)

The molecular model used in the studies reported here is based on one developed and used by Levy and coworkers.[33,34,41] This group used classical molecular dynamics to sample solvent configurations around a formaldehyde molecule, then performed electronic structure calculations to obtain the formaldehyde excitation energy in the static solvent field.[33] This method yielded a shift shift of 1900 $cm^{-1}$, agreeing with the experimental acetone shift. In other studies, the solvent shift for the vertical transition was computed directly from molecular dynamics by instantaneously switching the formaldehyde charges from the ground state charges to the excited state charges, and computing the change in the solvation energy. This method yielded a shift of about 4000 $cm^{-1}$,[41] twice as large as expected on the basis of experiments and quantum-mechanical calculations.

In Sec. II, we outline theoretical predictions that relate solvation in a polar, polarizable solvent to solvation in a polar, nonpolarizable solvent with the same total (static) dielectric constant, $\epsilon_0$. The type of linear response theory figures extensively in studies of quantum effects in solvation,[15–19,43–45] and also serves as the basis of Gaussian models for solvation.[46–48]

Dielectric continuum calculations with a molecular cavity are described in Sec. II B. The calculations required solving the Poisson–Boltzmann equation for the dielectric continuum response. We describe how these calculations were used to obtain $\Delta G$ and $\lambda$ parameters for the various solute charge sets, as well as to obtain solvent shifts in absorption and fluorescence spectra.

In Sec. III B, we discuss various methods of obtaining the charges for the ground state and excited states of formaldehyde. One method used previously for formaldehyde simulations,[33] natural population analysis (NPA), produces charges which are unrealistically large. Charge parameterization using electrostatic potential fitting (ESP), however, produces a more reasonable charge distribution and molecular dipole moment. The ESP charges also included enhancements due to favorable solvation by a dielectric continuum. In addition to the realistic ESP charge set, we describe two other charge sets. Charge set 2 is an NPA charge set used in

previous studies of formaldehyde solvation[19,33] and charge set 3 employs exaggerated ground and excited state charge distributions to serve as a drastic probe of the contributions of the solvent electric polarization modes.

In the simulations, the solute charges are fixed in each electronic state and do not respond to the local electronic environment provided by the solvent. This study does not use a polarizable solute in order to focus attention entirely on solvent polarizability. Polarizable solute models have typically been avoided in molecular simulations due to computational expense.[49] Efficient new approaches, including continuum models[50] and extended Lagrangian simulation algorithms for polarizable solutes,[51,52] have made polarizable solute simulations more tractable.

Simulation results for formaldehyde in water are presented in Sec. IV. The first results to be presented are for simulations with explicit molecular solvent. We compare the solvation energies obtained using polarizable solvent with energies from nonpolarizable solvent. Next we describe the continuum calculations using polarizable and nonpolarizable continuum solvents and a standard set of atomic radii. In the explicit solvent, reorganization energies in polarizable and nonpolarizable media are similar. In the continuum solvent, however, the reorganization energy for nonpolarizable solvent is substantially larger than that for polarizable solvent (consistent with theoretical analysis for linear response).

The solvation energies, with corresponding absorption and fluorescence solvent shifts, are compared to acetone experimental data in Sec. IV C. The results with the explicit molecular model designed to mimic the charge distribution in formaldehyde agree with experimental results for acetone, suggesting that the model is a realistic starting point for analyzing solvation energies.

Since reorganization energies in explicit solvent do not change significantly when solvent molecules are made polarizable, the molecular solvent is not behaving as a dielectric continuum. This, in turn, indicates that the solvent might not exhibit linear response, at least where electronic polarizability is concerned. We test the linearity of the solvent response by measuring the change in solvation energy for an overall scaling of the charges on the solute sites.

Finally, we discuss the differences between explicit molecular solvent simulation results and dielectric continuum solvent calculations. One important contribution to differences might be the solute radii that were used in continuum solvent calculations. In particular, the same values for the radii were used in continuum calculations for ground and excited state formaldehyde. Structural data from the simulations, however, indicate that the solvent cavity is smaller when the solute is in its highly polar ground state, and the cavity is larger for the less polar excited state. We investigate several methods for defining charge-dependent solute radii (see, for instance, Ref. 27), none of which can provide consistent agreement with the simulation data. To obtain more quantitative solvation energies from a calculation, it might be necessary to include nonlinear effects, such as charge-dependent radii for a solute molecule.

## II. THEORY

### A. Idealized cavity

The theoretical basis for understanding phenomena involving transitions between a pair of electronic states of a solute molecule immersed in a solvent is provided by Marcus theory.[1–4] This theory generally assumes that the solvent responds as a linear dielectric with fast and slow electric polarization modes. The fast modes represent quantum mechanical electronic polarization; the slow modes represent classical orientational degrees of freedom. This is a simplification, since high-frequency vibrational and librational modes—especially those arising within the first solvation shell—might require a more detailed quantum treatment, but it covers the essential aspects of the solvent response.

We will consider processes in which a solute molecule initially in state $i$ undergoes a transition to final state $f$. We focus on electronic transitions in which the dipole moment of the solute changes from $\mu_i$ in state $i$ to $\mu_f$ in state $f$. In real transitions, and for the transitions we simulate with molecular models, higher multipoles also change during the transition. We assume for now that the lowest order multipole, here the dipole, dominates the solvation response. Results of dielectric continuum calculations using the Poisson–Boltzmann equation, described in Sec. IV, indicate that this assumption is generally accurate for the formaldehyde models in this study.

The transition $f \leftarrow \imath$ occurs at an energy corresponding to that of a gas-phase transition shifted by a solvent contribution $\Delta E_{fi}$. The solvent shift can be written as the sum of two terms: $\Delta G_{fi}$, the solvent shift in the equilibrium free energies of solvation of the states $i$ and $f$, and $\lambda_{fi}$, termed the solvent reorganization energy and a measure of nonequilibrium solvation. Since $\lambda_{fi}=\lambda_{if}$, it is convenient to drop the subscript.

All the solvent polarization modes, fast modes and slow modes, contribute to the equilibrium term $\Delta G_{fi}$, but only the slow modes contribute to the nonequilibrium term $\lambda_{fi}$. The fast modes do not contribute to $\lambda_{fi}$ because their response is quantum mechanical and instantaneous, in effect renormalizing the quantum-mechanical energy levels of the solute states.

Continuum theory can be used to relate the solvation parameters $\Delta G$ and $\lambda$ to properties of the solute and solvent. These results are summarized in the following standard equations:

$$\Delta E_{fi}=\Delta G_{fi}+\lambda_{fi}, \tag{1a}$$

$$\Delta G_{fi}=-\tfrac{1}{2}(\alpha_0+\alpha_\infty)(\mu_f^2-\mu_i^2)=-\Delta G_{if}, \tag{1b}$$

$$\lambda_{fi}=\tfrac{1}{2}\alpha_0(\mu_f-\mu_i)^2=\lambda_{if}. \tag{1c}$$

These equations lead to operational definitions of $\Delta G_{fi}$ and $\lambda_{fi}$ in terms of $\Delta E_{fi}$ and $\Delta E_{if}$, which can be measured from simulations directly

$$\Delta G_{fi}=\tfrac{1}{2}(\Delta E_{fi}-\Delta E_{if}); \tag{2a}$$

$$\lambda_{fi}=\tfrac{1}{2}(\Delta E_{fi}+\Delta E_{if}). \tag{2b}$$

TABLE I. The factor $\lambda_{pol}/\lambda_{nonpol}$ for TIP4P-FQ water is calculated using $\epsilon_0=80$ and $\epsilon_\infty=1.59$.

| Solute | $\lambda_{pol}/\lambda_{nonpol}$ |
|---|---|
| Monopole | 0.62 |
| Dipole | 0.71 |

By symmetry, $\lambda_{if}=\lambda_{fi}$.

The parameters $\alpha_0$ and $\alpha_\infty$ appearing in Eq. (1) correspond to the solvent polarizability arising from low-frequency modes and from high frequency modes. For dipole solvation, these parameters are given by a product of a cavity-size term $F_{cav}$ and a second term dependent on the static dielectric constant $\epsilon_0$ and the high-frequency dielectric constant $\epsilon_\infty$[53]

$$\alpha_0=F_{cav}\times\left[\frac{2(\epsilon_0-1)}{2\epsilon_0+1}-\frac{2(\epsilon_\infty-1)}{2\epsilon_\infty+1}\right], \tag{3a}$$

$$\alpha_\infty=F_{cav}\times\frac{2(\epsilon_\infty-1)}{2\epsilon_\infty+1}. \tag{3b}$$

These theoretical predictions can be used to relate solvation energies in a polarizable solvent to solvation energies in a nonpolarizable solvent. We assume that both solvents have an identical equilibrium response and the same static dielectric constant $\epsilon_0$. It follows from Eq. (1) that $\Delta G$ as measured in either solvent will be the same. The reorganization energies will be different in the two solvents, however, because the solvents have different optical dielectric constants $\epsilon_\infty$. For the nonpolarizable solvent, $\epsilon_\infty=1$, whereas $\epsilon_\infty>1$ for a polarizable solvent. Analysis of Eq. (3) indicates that $\lambda$ in a polarizable solvent will be smaller than $\lambda$ in a nonpolarizable solvent. The exact ratio depends on $\epsilon_\infty$ of the polarizable solvent. For the polarizable FQ water model,[27] $\epsilon_\infty=1.592$, which is close to the experimental value of 1.78 for real water. The ratio $\lambda_{pol}/\lambda_{nonpol}$ for FQ water is 0.71.

### B. Continuum calculations for a molecular cavity

The theoretical predictions in the previous section are based on an idealized solute with a spherical shape and a point dipole at its center. It is necessary to consider a solute with a molecular shape and a realistic charge distribution to make accurate predictions for real molecules. Although it is possible to extend the analytic approach to geometries more complicated than a sphere,[54,55] for full generality it is worthwhile to employ a numerical calculation to solve the Poisson–Boltzmann equation for the polarization of a continuum dielectric fluid surrounding a molecular solute. The Poisson–Boltzmann solver PBF,[56] which solves the equation using a three-dimensional finite element numerical method, was used for this purpose.

The program PBF was modified in order to obtain values for the average energy gaps $\Delta E_{21}$ and $\Delta E_{12}$ between a solute ground state (labeled 1) and excited state (labeled 2). The energy gaps were obtained by first solving for the solvent polarization charge on the surface defining the interface between the continuum solvent and the solute molecule in electronic state 1. Denoting the solute charges and charge locations as $\{Q_1^i\}$ and $\{R_i\}$, and denoting the surface charge at position $r$ on the surface as $q_1(r)$, the reaction field solvation energy for solute state 1 is

$$E_1^{rf}=\tfrac{1}{2}\sum_i Q_1^i\int_S dr\ q_1(r)/|r-R_i|. \tag{4}$$

The integration is over the surface $S$ between the solute and the dielectric continuum. The energy gap between state 1 and state 2 is then obtained by instantaneously switching the solute charges from $\{Q_i^1\}$ to $\{Q_i^2\}$ while holding the solvent surface charges fixed,

$$\Delta E_{21}=\sum_i (Q_2^i-Q_1^i)\int_S dr\ q_1(r)/|r-R_i|. \tag{5}$$

In the calculation described above, the solvent charge distribution is fixed during the electronic transition. This means that the continuum solvent represents a nonpolarizable dielectric, $\epsilon_\infty=1$. Calculating $\Delta E$'s in a polarizable solvent requires additional steps, as described below.

Calculating $\Delta E$ for a polarizable solvent mimicking FQ water ($\epsilon_0=80.37$ and $\epsilon_\infty=1.592$) requires two sets of calculations of $\Delta E_{21}$ and $\Delta E_{12}$ for each electronic transition. In the first calculation, the solvent dielectric constant is set to 80.37, corresponding to full dielectric response. In the second calculation, a dielectric constant of 1.592 corresponding to the value of the optical dielectric constant is employed in order to measure the contribution to the energy gap from the electronic polarization modes of the solvent. In both cases, however, the entire polarization of the dielectric continuum is treated as slow and classical.

For a clear notation, let a single prime ($'$) denote a PBF calculation done using $\epsilon_{exterior}=80.37$, and let a double prime ($''$) denote a PBF calculation using $\epsilon_{exterior}=1.592$. The singly and doubly primed quantities treat all modes as nonpolarizable. Unprimed quantities are understood to treat polarizable modes correctly: they make no contribution to $\lambda$.

The values $\Delta E'_{21}$, $\Delta E'_{12}$, $\Delta E''_{21}$, and $\Delta E''_{12}$ are computed directly from Eq. (5) using PBF. The reaction field solvation energies $E_1^{rf'}$, $E_2^{rf'}$, $E_1^{rf''}$, and $E_2^{rf''}$ are computed directly from Eq. (4). Because a dielectric continuum assumes a harmonic bath, and energies and free energies differences are the same for a harmonic bath, the reaction field energies are also free energies of solvation. For example, $\Delta G'_{21}=E_2^{rf'}-E_1^{rf'}$. This provides a consistency check for the calculation, because, for example, $\Delta G'_{21}$ is also related to the difference between $\Delta E'_{21}$ and $\Delta E'_{12}$

$$\Delta G'_{21}=(\Delta E'_{21}-\Delta E'_{12})/2=E_2^{rf'}-E_1^{rf'},$$

$$\Delta G''_{21}=(\Delta E''_{21}-\Delta E''_{12})/2=E_2^{rf''}-E_1^{rf''}. \tag{6}$$

The free energy difference $\Delta G_{21}$ is the same as $\Delta G'_{21}$ because polarizable modes contribute fully to $\Delta G$.

The correct reorganization energy $\lambda$ can be obtained from $\lambda'$ and $\lambda''$. We calculate the reorganization energies $\lambda'$ and $\lambda''$ using the formulas

$$\lambda' = (\Delta E'_{21} + \Delta E'_{12})/2,$$
$$\lambda'' = (\Delta E''_{21} + \Delta E''_{12})/2. \tag{7}$$

Since the fast and slow modes can be treated as uncoupled normal modes,[19] their contribution to λ is additive. Furthermore, λ′ contains contributions from all the modes, whereas λ″ is only the contribution from polarizable modes (which are treated as nonpolarizable in the PBF calculation). Therefore, the correct λ can be obtained as

$$\lambda = \lambda' - \lambda''. \tag{8}$$

After the correct value of λ has been obtained, the energy gaps $\Delta E_{21}$ and $\Delta E_{12}$ can be obtained using $\Delta E_{21} = \lambda + \Delta G_{21}$.

The parameters that complete the specification of the continuum calculation are the solute charge distributions, which will be described in Sec. III B, and the solute cavity. The molecular surface that defines the solute cavity is defined by rolling a sphere with a probe radius around solvent atoms with defined atomic radii. The PBF default parameters were chosen[56] and are listed in Table IV. The interior dielectric constant of the solute, $\epsilon_{\text{interior}}$, was taken to be 1 because the solute in the simulations is nonpolarizable. Two values were used for the exterior dielectric constant. The first, $\epsilon_{\text{exterior}}$, is the default static dielectric constant used by PBF, 80.37. The second, $\epsilon'_{\text{exterior}}$, is the optical dielectric constant of the FQ model, 1.592.

### C. Continuum calculations for a charge-dependent molecular cavity

Conventional calculations of the solvation response of a dielectric continuum surrounding a solute use a single set of radii to characterize the solute, regardless of the charge state of the solute. Although this is a convenient approach, it is also an approximation. Several studies have shown that the effective radius of a solute can depend on its charge distribution.[57] A solute that is highly polar will attract solvent molecules and has an effective radius that is smaller than the effective radius of a less polar solute.

As discussed elsewhere, the charge-dependence of the solute cavity size introduces nonlinearity into the solvent response.[19] We describe here how this type of nonlinear effect can be included in dielectric continuum calculations by employing a molecular-shaped cavity that depends on the solute charge.

First, we simplify the discussion by considering a solvent with no electronic polarizability. The solvent shift in the absorption spectrum is $E_{21}$, and the shift in the fluorescence spectrum is $E_{12}$. During the absorption experiment, the solvent is essentially static and equilibrated to the ground state of the solute. This indicates that the molecular cavity used in a continuum calculation of $E_{21}$ should correspond to the ground state cavity. Similarly, the molecular cavity used in a continuum calculation of $E_{12}$ should correspond to the excited state cavity. Once $E_{21}$ and $E_{12}$ are known, $G_{21}$ is defined operationally as $(E_{21}-E_{12})/2$, and λ is defined operationally as $(E_{21}+E_{12})/2$.

To calculate $G_{21}$ and λ for a polarizable solvent, the same course outlined in Sec. II B is followed. Calculations are performed with two nonpolarizable continuum solvents, one with $\epsilon_0 = 80.37$, and the other with a continuum solvent with $\epsilon_0 = 1.592$. The free energy difference $G_{21}$ is obtained from the calculation with $\epsilon_0 = 80.37$. The reorganization energy λ is obtained as the difference between the λ values of the two continuum solvents. The absorption and fluorescence shifts $E_{21}$ and $E_{12}$ are then obtained as $\lambda + G_{21}$ and $\lambda - G_{21}$, respectively.

## III. MODEL

### A. Water

Simulation results are reported for four treatments of the aqueous solvent: polarizable TIP4P-FQ,[27] nonpolarizable MQ,[19] nonpolarizable TIP4P,[28] and a hybrid FQ-MQ model[19] in which the conformations are taken from a TIP4P-FQ simulation but the fixed MQ charges are used to compute energies.

In the FQ model, the water molecules are made polarizable by allowing charge to flow between sites on each molecule. The charges are always in equilibrium with the local electric environment.

To simulate an electronic transition with the FQ model, the solvent charges are first equilibrated to the initial solute dipole $\mu_i$ and the total energy of the system is calculated. Then the solute state is changed from $i$ to $f$, with solute dipole $\mu_f$, and the charges are reequilibrated to the final solute state. The total energy of the system is again calculated. In the Appendix, we show that this treatment is equivalent to a quantum mechanical treatment for the electronic polarization.

### B. Formaldehyde

The formaldehyde model is based on work by Levy and co-workers.[33,34,41] The geometry of the rigid molecule is specified by $R_{CO} = 1.184$ Å, $R_{CH} = 1.093$ Å, and $\angle HCH = 115.5°$. A single set of Lennard-Jones parameters and several sets of charge parameters represent formaldehyde in its ground and excited states.

#### *1. Lennard-Jones parameters*

Standard combining-rule $\epsilon$ and $\sigma$ Lennard-Jones parameters were adopted from Ref. 41 and are the same parameters used in our previous study.[19] Since the water models have different Lennard-Jones parameters, the combining rules yield formaldehyde–water interactions that depend on the water model, as has been discussed elsewhere.[19]

A more detailed model of formaldehyde would allow ground state and excited state Lennard-Jones parameters to differ. Compared to the ground state, the excited state molecule has excess electron density in antibonding $\pi^*$ orbitals and is expected to have a larger Lennard-Jones diameter $\sigma$. Also, because the gap to even more highly excited states is small relative to the gap from the ground state, the polarizability of the excited state is expected to be larger than that of the ground state. This would imply a larger energy param-

eter $\epsilon$ as well. Herman and Berne have investigated the solvation of a $Br_2$ molecule in Ar in which the Lennard-Jones energy parameter for Br–Ar interactions is coupled to the $Br_2$ bond length.[58] Their simulations showed that the distance dependence in $\epsilon$ had a significant effect on the excitation frequency for the transition from the ground vibrational state to first excited state of solvated $Br_2$. A theoretical treatment of the same type of system clearly indicates the importance of the Lennard-Jones parameters in determining solvent contributions to vibrational frequency shifts and dephasing.[59]

Given that Lennard-Jones parameters should depend on the electronic state of a molecule, and that solute–solvent interactions depend on the Lennard-Jones parameters, it might be necessary to include a change in the Lennard-Jones parameters to attain a quantitative agreement with experiment. Our primary concern in these studies, however, is the polarization contribution to solvent shifts and differences between shifts from molecular solvents and continuum solvents. This study, therefore, does not include models in which the formaldehyde Lennard-Jones parameters depend on the electronic state.

### 2. Charge parameters

Experimental measurements of formaldehyde give a gas-phase ground-state dipole moment of 2.3 D[60,61] and an excited state dipole moment of 1.57 D.[62,63] These two measurements are insufficient to characterize the atomic charges, and also do not reflect charge enhancements arising from solvation in a dielectric. *Ab initio* calculations were used to develop realistic charge sets for formaldehyde in water. These calculations all used a 6-31 G** basis set. Two commercially available electronic structure packages were used to perform the calculations, GAUSSIAN 92[64] and PS-GVB.[65]

GAUSSIAN 92 and PS-GVB generate solvated charges by placing a molecule in a cavity in a dielectric continuum solvent, allowing the molecular charges to polarize the medium, introducing a term in the electronic Hamiltonian representing the interaction energy between the solute and the solvent polarization, and iterating until self-consistency is reached. GAUSSIAN 92 uses an ellipsoidal cavity for the molecule. PS-GVB uses a more realistic cavity enclosed by the molecular surface (Richards definition),[66] and the surface polarization charge is determing by solving the Poisson–Boltzmann equation. The solvent dielectric constant was 80 in all cases. Because the representation of the solvent cavity is more realistic with PS-GVB than with GAUSSIAN 92, we used PS-GVB to calculate solvated charges for the ground state molecule.

The Poisson–Boltzmann solver used by PS-GVB, termed PBF, solves the Poisson–Boltzmann equation for the surface charges using a finite element algorithm. The solvation energy provided by PS-GVB and PBF is the sum of three terms: (1) the reaction field energy, $E_{\mathrm{rf}}$; (2) a surface tension energy; and (3) the energetic cost of polarizing the solute molecule, an unfavorable contribution due to the change in the electronic structure upon solvation. The surface tension term is simply proportional to the surface area of the solute cavity. Using the default parameters, which are listed in Table IV, this term is 1.90 kcal/mol for the fixed formaldehyde geometry. GAUSSIAN 92 was used to obtain excited state charges. The gas-phase charges were then scaled to account for the enhancement from solvation.

Electrostatic potential fitting (ESP) produced the final charge parameters from the electronic structure. Other methods, such as natural population analysis (NPA)[67] and Mulliken population analysis (MPA) gave solute charges that were much too large. We describe charge sets as the triple $(Q_{\mathrm{O}}, Q_{\mathrm{C}}, Q_{\mathrm{H}})$ in units of $|e|$.

### 3. Ground state charges

A PS-GVB gas phase calculation provided ESP fit charges of (−0.407, 0.422, −0.0075) and a dipole of 2.27 D. This dipole moment agrees well with the experimental value of 2.3 D.[60,68] The charges obtained from MPA, (−0.363, 0.189, 0.087), give a larger dipole moment of 2.55 D and do not agree as well with the experimental data.

When the solvation term was added, the dipole was enhanced by about 30%. We obtained ESP charges of (−0.500, 0.476, 0.012) and a dipole moment of 2.91 D. The charges (−0.438, 0.203, 0.118) were obtained from MPA, giving a dipole moment of 3.15 D. Since the gas-phase results suggest that the MPA charges are too large, the ESP charge set was selected for ground state charge set 1. The total solvation energy reported by PS-GVB using default parameters was −2.9 kcal/mol. This total comprises a favorable reaction field energy of −6.0 kcal/mol, a solute polarization energy cost of 1.17 kcal/mol, and the previously mentioned surface tension cost of 1.90 kcal/mol.

For comparison with the PS-GVB results, we also report results using GAUSSIAN 92. At the RHF level, the charge set obtained using ESP[69] was (−0.477, 0.494, −0.0085), giving a dipole moment of 2.66 D. The RHF results predict a larger dipole than predicted by PS-GVB, probably because the generalized valence bond method employed by PS-GVB incorporates some electron correlation and is therefore at a higher level of theory than RHF. With CISD, which includes electron correlation (unlike RHF), the ESP charges are (−0.427, 0.481, −0.027), and the dipole moment is 2.28 D. This final value is virtually identical to the PS-GVB gas-phase result.

### 4. Excited state charges

For the fixed geometry of the ground state, we used GAUSSIAN 92 with CIS to obtain the excited state ESP charge set (−0.039, −0.407, 0.223) and a dipole of 1.47 D. The excited state dipole moment is close to the experimental value of 1.57 D.[62,63] To obtain solvated charges, we scaled the ESP fit charges by the factor 1.28, the ratio of the solvated to gas-phase dipole for ground state formaldehyde as calculated by PS-GVB. This yields a charge set of (−0.050, −0.521, 0.2855) and a dipole moment of 1.88 D for excited state charge set 1.

Rather than scaling the gas-phase charges to obtain the solution-phase charges, it would have been possible to use

GAUSSIAN 92 to predict the solution-phase charges based on the reaction field generated inside an ellipsoidal cavity. This would have introduced two types of cavities in the solvated charge distributions—a molecular cavity for the ground state and an ellipsoidal cavity for the excited state—and for this reason we chose to perform the scaling instead.

A likely source of error in this scaling procedure for the excited state charges is that the dipole moment enhancement should scale with the polarizability, and the excited state formaldehyde is expected to have a larger polarizability than the ground state molecule. It might have been appropriate to scale the factor of 1.28 by a second factor equal to the ratio of the excited state to ground state polarizability.

A second, less likely source of error is our use of a uniform scaling factor. In the ground state, the charges do not scale uniformly from the gas phase to the solvated state. The magnitude of the charge on the oxygen increases by 23%, the magnitude of the charge on carbon increases by 13%, and the charge on hydrogen changes sign, all to increase the dipole moment by 28% from 2.27 to 2.91 D. These details of charge flow are not captured by the overall scaling of excited state charges by the net factor of 1.28. To test the effect of net scaling of charges, we compared the dielectric continuum solvation energies of two models for ground state formaldehyde. The first model had the ESP liquid-state charges and a dipole moment of 2.91 D. The second model had the ESP gas-phase charges scaled by the factor 1.28, also giving a dipole moment of 2.91 D. The solvation energy in the first case was −6.0 kcal/mol, and in the second case was −6.1 kcal/mol. Thus we do not expect that the overall scaling of charges is a large source of error.

### 5. Comparison to previous parameterizations

Several charge sets have been developed for formaldehyde. Blair *et al.* reported[33] that an RHF calculation using a 6–31 G* basis yields NPA charges of (−0.576, 0.331, 0.123), and a dipole moment of 3.97 D. This dipole is 70% larger than the experimental value of 2.3 D. This charge distribution is the ground state of charge set 2.

Levy and co-workers report two calculations of charges for the $^1A_2$ excited state of formaldehyde. Using a 6–31 G* basis with ROHF[70] at the ground state geometry, NPA gives a charge set of (−0.238, −0.143, 0.191) and a dipole moment of 2.42 D.[33] In a second calculation, the gas phase charges were determined using the optimized ROHF excited state geometry.[41] Here, the charge set found by NPA is (−0.280, −0.040, 0.160), giving a dipole of 2.49 D. This charge distribution is the excited state of charge set 2. Note that these dipole moments are much larger than the experimentally determined gas phase dipole moment of 1.57 D.[62,63]

### 6. Simulation parameters

We performed simulations with three pairs of ground state and excited state charge distributions. Charge set 1 employs realistic, solvated charges from ESP fitting. In this set, the ground state dipole moment is 2.91 D and the excited state dipole moment is 1.88 D.

TABLE II. Charge sets for formaldehyde.

| | Charges ($\|e\|$) | | | $\mu_y$ (D) | $Q_{xx}$[a] | $Q_{yy}$ | $Q_{zz}$ |
|---|---|---|---|---|---|---|---|
| | O | C | H | | | | |
| Set 1 | | | | | | | |
| $^1A_1$ | −0.500 | 0.476 | 0.012 | 2.91 | 0.734 | −1.406 | 0.672 |
| $^1A_2$ | −0.050 | −0.521 | 0.2855 | 1.88 | 0.850 | −0.238 | −0.612 |
| Set 2 | | | | | | | |
| $^1A_1$ | −0.577 | 0.331 | 0.123 | 3.97 | 1.145 | −1.660 | 0.515 |
| $^1A_2$ | −0.280 | −0.040 | 0.160 | 2.49 | 0.830 | −0.840 | 0.010 |
| Set 3 | | | | | | | |
| $^1A_1$ | −0.872 | 0.500 | 0.186 | 6.00 | 1.731 | −2.509 | 0.778 |
| $^1A_2$ | −0.112 | −0.016 | 0.064 | 1.00 | 0.332 | −0.336 | 0.004 |

[a]Nonzero elements of the traceless quadrupole tensor are given in units of $|e|$ Å$^2$. The formaldehyde is in the $x-y$ plane with the CO bond along the $y$-axis.

Charge set 2, based on a previous parameterization using a gas-phase calculation and NPA,[33,41] has a ground state dipole moment of 3.97 D and an excited state dipole moment of 2.49 D. This charge set was also used in a previous study involving a polar, polarizable molecular solvent.[19]

In charge set 3, the ground state molecule has an artificially enhanced dipole moment of 6 D, and the excited state molecule has a reduced dipole moment of 1 D. These charge distributions magnify the differences in solvation energy for the two solute electronic states. The 6 D ground state was obtained by scaling the charge set 2 ground state by a factor of 1.51, and the 1 D excited state charges were obtained by scaling the charge set 2 excited state by a factor of 0.402.

The charge distributions for these three sets are displayed in Table II. Dipole moments and reaction field solvation energies, as calculated by PBF using the default parameters listed in Table IV, are listed in Table III. As described in Sec. III B 2, the reaction field energy adds with the hydrophobic interaction energy and the solute self-polarization energy to give the total solvation energy.

In a dielectric continuum, the reaction field solvation energy $E_{\mathrm{rf}}$ for a point dipole with moment $\mu$ in a fixed cavity scales with $\mu^2$ [see Eq. (1b)]. Thus if the solute dipole pro-

TABLE III. Dipoles and reaction field energies for formaldehyde models.

| | $\mu$ (D) | $E_{\mathrm{rf}}$[a] (kcal/mol) | $E_{\mathrm{rf}}/\mu^2$ (kcal/mol D$^2$) |
|---|---|---|---|
| Set 1 | | | |
| $^1A_1$ | 2.91 | −6.0 | 0.71 |
| $^1A_2$ | 1.88 | −3.6 | 1.02 |
| Set 2 | | | |
| $^1A_1$ | 3.97 | −10.9 | 0.69 |
| $^1A_2$ | 2.49 | −4.4 | 0.71 |
| Set 3 | | | |
| $^1A_1$ | 6.00 | −25.0 | 0.69 |
| $^1A_2$ | 1.00 | −0.7 | 0.70 |

[a]$E_{\mathrm{rf}}$ is the reaction field contribution to the solvation energy as determined by the Poisson–Boltzmann equation for a dielectric continuum.

TABLE IV. Parameters for dielectric continuum calculations.

| Radii (Å) | |
|---|---|
| O | 1.60 |
| C | 1.949 15 |
| H | 1.15 |
| Probe | 1.53 |
| Dielectric constants | |
| $\epsilon_{\text{interior}}$ | 1 |
| $\epsilon_{\text{exterior}}$ | 80.37 |
| $\epsilon_{\text{exterior}'}$ | 1.592 |

vides the dominant contribution to the solvation energy for the six formaldehyde charge distributions we consider, the ratio $E_{\text{rf}}/\mu^2$ should be a constant.

The values of $E_{\text{rf}}/\mu^2$ are listed in Table III. It is evident that all the values lie in a narrow range 0.69–0.71 kcal/mol $D^2$, except for the excited state from charge set 1. For this molecule with dipole moment 1.88 D we find that $E_{\text{rf}}/\mu^2=1.0$ kcal/mol $D^2$. This might indicate that there is a significant quadrupolar contribution to the solvation energy for this charge distribution. Indeed, an examination of the charge distribution for the excited state of set 1 indicates that the charge on the H sites is quite large, $q_{\text{H}}=0.2885|e|$, and there is a large difference between the quadrupole of the ground and excited state for this set of charges.

The quadrupole moments for each charge set are given in Table II. These moments correspond to elements of the traceless quadrupole tensor,

$$Q_{jk}=\sum_{\alpha} Q_{\alpha}(3r_j^{(\alpha)}r_k^{(\alpha)}-\delta_{jk}|r^{(\alpha)}|^2), \tag{9}$$

where $Q_\alpha$ is the charge of site $\alpha$, $r^{(\alpha)}$ is the position of site $\alpha$, and $r_j^{(\alpha)}$ and $r_k^{(\alpha)}$ are the $x$, $y$, and $z$ components of $r^{(\alpha)}$. The indices $j$ and $k$ each take values $x$, $y$, and $z$. In computing the quadrupoles, the formaldehyde C was at the origin, the molecule was in the $x-y$ plane, and the molecular dipole was along the $y$ axis. The only nonzero elements of the quadrupole tensor for the planar formaldehyde molecule in this orientation are $Q_{xx}$, $Q_{yy}$, and $Q_{zz}$. For the charge sets 2 and 3, the quadrupole moments of the ground state are larger than the quadrupole moments of the excited state. In charge set 1, however, the quadrupole moments of the ground state are not much larger than the moments of the excited state. Furthermore, the component $Q_{xx}$ is even larger in the excited state than in the ground state and contributes to the large ratio $E_{\text{rf}}/\mu^2$ for charge set 1.

### C. Simulation method

The simulation box used for all the molecular simulations was 18.6 Å on a side and contained 209 water molecules and a single formaldehyde molecule. Periodic boundary conditions were used with Ewald sums for the electrostatic interactions.[49] The time step was 1 fs and molecules were kept rigid using the RATTLE algorithm.[49,71]

Solvent shifts were calculated for polarizable TIP4P-FQ and the non-polarizable TIP4P-FQ/MQ, TIP4P-MQ, and TIP4P as described previously.[19] One source of difference between the energy gaps observed in polarizable versus nonpolarizable water is a difference in solvation structure in the two solvents. To test this effect, the FQ/MQ simulations use configurations from FQ trajectories but calculate energy gaps using fixed-charge MQ parameters.[19]

When performing the simulations for each of the charge sets and each of the solvents, we used at least 40 ps of equilibration before collecting statistics. Data collection lasted 50 ps for charge set 1 and 100 ps for charge sets 2 and 3.

## IV. RESULTS AND DISCUSSION

### A. Comparison of polarizable and nonpolarizable molecular solvent

As indicated in Table V, we performed simulation with a variety of solvent models: the polarizable FQ model and nonpolarizable FQ/MQ, MQ, and TIP4P models. The results reported in Table V make clear that the polarizability of the solvent has only a minor effect on solvation and reorganization energies.

This result is expected for $\Delta G_{21}$, an equilibrium energy that should depend only on the static dielectric properties of a solvent. For charge set 1, the most realistic charge set, the values are 3.7 and 3.9 kcal/mol. For charge set 2, $\Delta G_{21}$ ranges from 7.3–7.5 kcal/mol depending on the solvent model. The range for charge set 3 is 30.1–31.7 kcal/mol. These ranges correspond to roughly 5% relative to $\Delta G_{21}$ itself. The agreement of the results for $\Delta G_{21}$ also provides assurance that the simulation results have converged.

It is surprising, however, that the values obtained for the reorganization energy $\lambda$ are also relatively independent of solvent polarizability. For charge set 2, the values are separated by 0.4 kcal/mol, roughly the magnitude of the statistical error in $\lambda$. For charge set 3, the difference is 2.9 kcal/mol, or about 10% of the simulation value of 25 kcal/mol for the FQ model of water.

The difference between the theoretical prediction (solvent polarizability decreases $\lambda$) and the simulation results (solvent polarizability does not affect $\lambda$) cannot be ascribed to the charge distributions used for the formaldehyde solute. If that had been the cause of the difference, then the continuum results (described in the following section) would also have demonstrated this anomolous behavior. Thus we are confident that the disagreement between theory and simulation is due to an inherent failure of the linear response theory to describe adequately the solvation response of polarizable models for water.

### B. Comparison of polarizable and nonpolarizable continuum solvent

Results for three continuum solvents are presented in the right half of Table V. The first, labeled ''pol,'' refers to a polarizable solvent designed to mimic liquid water. This continuum solvent has a static dielectric constant of 80.37 and an optical dielectric constant of 1.592, the same as the polarizable FQ solvent. The second continuum solvent, which is

TABLE V. Table of energies, all in kcal/mol.

| | Simulation | | | | Dielectric continuum[a] | | |
|---|---|---|---|---|---|---|---|
| | EQ | FQ/MQ | MQ | TIP4P | Pol[b] | Nonpol | Nonpol |
| $\epsilon_0$ | 80 | ~80 | ~80 | 53 | 80.370 | 80.370 | 1.592 |
| $\epsilon_\infty$ | 1.592 | 1 | 1 | 1 | 1.592 | 1 | 1 |
| Charge set 1 | | | | | | | |
| $\Delta E_{21}$ | 6.4 | 7.0 | | | 4.31 | 5.20 | 1.70 |
| $\Delta E_{12}$ | −0.9 | −0.7 | | | −0.55 | 0.34 | 0.07 |
| $\Delta G_{21}$ | 3.7 | 3.9 | | | 2.43 | 2.43 | 0.82 |
| λ | 2.8 | 3.2 | | | 1.88 | 2.77 | 0.89 |
| Charge set 2 | | | | | | | |
| $\Delta E_{21}$ | 10.2 | 10.7 | 10.5 | 10.3 | 7.64 | 8.18 | 2.68 |
| $\Delta E_{12}$ | −4.3 | −4.3 | −4.2 | −4.7 | −5.38 | −4.82 | −1.58 |
| $\Delta G_{21}$ | 7.3 | 7.5 | 7.4 | 7.5 | 6.51 | 6.51 | 2.13 |
| λ | 3.0 | 3.2 | 3.2 | 2.8 | 1.13 | 1.68 | 0.55 |
| Charge set 3 | | | | | | | |
| $\Delta E_{21}$ | 55.7 | 55.6 | 59.4 | | 36.08 | 41.77 | 13.62 |
| $\Delta E_{12}$ | −6.2 | −4.5 | −4.0 | | −12.56 | −6.86 | −2.23 |
| $\Delta G_{21}$ | 31.0 | 30.1 | 31.7 | | 24.32 | 24.32 | 7.93 |
| λ | 24.8 | 25.6 | 27.7 | | 11.76 | 17.46 | 5.70 |

[a]From PBF with same sized cavity for the ground and excited states.
[b]Obtained from PBF using the data from $\epsilon_0=80.37$ and 1.592 with $\epsilon_\infty=1$ as described in Sec. II B.

labeled ''nonpol,'' is designed to mimic nonpolarizable water. It has a static dielectric constant of 80.37 and an optical dielectric constant of 1. The third continuum solvent is also labeled ''nonpol.'' This solvent has a static dielectric constant of 1.592 and an optical dielectric constant of 1. This solvent is not meant to represent water, but the results for this model were required in order to determine the solvation energies for the polarizable continuum solvent. The calculations used to obtain the results for the polarizable continuum solvent were described in as described in Sec. II B.

The theory presented in Sec. II indicates that λ for a polarizable solvent with $\epsilon_0=80.370$ and $\epsilon_\infty=1.592$ should be a fraction 0.71 of λ for a nonpolarizable solvent with $\epsilon_0=80.370$ and $\epsilon_\infty=1$. The reorganization energies for each of the three charge sets for these two types of continuum solvent are listed in the right half of Table V.

As predicted by the theory, the ratios we obtain are very close to 0.71. For charge set 1, the ratio is (1.88/2.77), or 0.68. The ratio for charge set 2 is $(1.13/1.68)=0.67$, and that for charge set 3 is $(11.76/17.46)=0.67$. The small deviation from the theoretical prediction reflects the small difference between the charge distribution of a molecule like formaldehyde and the charge distribution used for the theoretical prediction, a point dipole at the center of a spherical cavity.

### C. Comparison with experimental solvent shifts for acetone

It is difficult to determine the solvent shift for the formaldehyde absorption in water due to oligomer formation. For acetone, the experimental line is very broad with the maximum shifted from the gas-phase line by 6 kcal/mol.[29] Only the first two charge sets are compared to experimental results, since the third charge set has exaggerated dipoles for formaldehyde.

#### *1. Charge set 1*

Charge set 1, with realistic solvated formaldehyde charges, yields a solvent shift of 6.4 kcal/mol in the absorption line. This shift is quite close to the experimental value for acetone. The shift in the simulation contains only the reaction field contribution. The hydrophobic interactions are assumed to be equivalent for the ground and excited states and therefore make no net contribution to the shift. The solute self-polarization energy should contribute to the shift. We have not, however, included this term in the simulations. From the electronic structure calculation for the ground state, this self-energy is known to be 1.17 kcal/mol. It can be estimated for the excited state by assuming that it is proportional to the square of the change in the dipole moment upon solvation. That is, the self-polarization cost for the excited state is roughly

$$\frac{(1.88-1.47)^2}{(2.91-2.27)^2}\times 1.17 \ \text{kcal/mol} \tag{10}$$

or 0.5 kcal/mol. This would decrease the solvent shift from 6.4 to 5.9 kcal/mol.

The prediction for the solvent shift using the continuum solvent model is 4.3 kcal/mol. This shift is 33% smaller than the simulation result. This indicates that the dielectric continuum model does not provide sufficient solvation. The solvent shift is also smaller than the experimental shift for acetone.

TABLE VI. Solvation energies are scaled by dipole moments.

| | $\Delta G_{21}/(\mu_2^2-\mu_1^2)$[a] | | $\lambda/(\mu_2-\mu_1)^2$ [b] | |
|---|---|---|---|---|
| Charge Set | FQ | Diel. Cont. | FQ | Diel. Cont. |
| 1 | 0.75 | 0.49 | 2.6 | 1.8 |
| 2 | 0.76 | 0.68 | 1.4 | 0.52 |
| 3 | 0.89 | 0.70 | 1.0 | 0.47 |

[a]All values are in units kcal/mol $D^2$.
[b]All values are in units kcal/mol $D^2$.

#### 2. Charge set 2

Simulations using charge set 2 (NPA charges) predict a solvent shift of about 10 kcal/mol from simulation. This agrees very well with the previous simulation results of Levy and co-workers using the same charge set,[41] but is about 70% larger than the results from the ESP charges and also much larger than the experimental acetone shift. The dipole moments in the NPA charge set are about 35% larger than the dipoles in the ESP charge set. Since absorption energies scale as (dipole),[2] a difference of about 80% in solvation energies is predicted. We also note that electronic structure calculations for configurations derived from simulations using the NPA charge set produced a solvent shift close to 5 kcal/mol.[33] These comparisons all suggest that NPA charges are too large, and that ESP charges provide a more realistic description of molecular interactions.

The continuum result for the solvent shift for charge set 2 is 7.6 kcal/mol. This is 25% smaller than the simulation results, again indicating that the continuum solvent provides insufficient solvent response compared to a molecular solvent.

### D. Comparison of molecular solvent with continuum solvent

Solvation energy differences $G_{21}$ and reorganization energies $\lambda$ have been obtained for the various charge sets. The values from molecular simulations and dielectric continuum calculations are compared below. The agreement of solvation energies with linear response predictions is also investigated, with results reported in Table VI.

#### 1. Free energies of solvation

In Table V, solvation energy differences $\Delta G_{21}$ are presented for the three formaldehyde charge sets. In each charge set, the excited state is less polar than the ground state and therefore less favorably solvated, making $\Delta G_{21}$ a positive quantity.

The value for $\Delta G_{21}$ predicted by continuum theory using the Poisson–Boltzmann equation is generally smaller than the simulation results. For charge set 1, the continuum prediction is 65% of the simulation results (2.4 vs 3.7 kcal/mol). It is 90% as large for charge set 2 and 80% as large for charge set 3. These errors indicate a possible failure of the continuum theory. The average absolute error for charge sets 1 and 2 is 1 kcal/mol, typical of comparisons between continuum calculations and molecular simulations. The absolute error for charge set 3 is much larger, almost 7 kcal/mol, but these charges are unrealistically large.

The continuum calculation employs a molecular-shaped cavity with an internal charge distribution rather than a point dipole at the center of a spherical cavity. This type of calculation includes contributions from solute–solvent interactions beyond dipole order in the multipole expansion. The contribution of the terms beyond dipole order can be investigated through the scaling of the solvation energy difference $\Delta G_{21}$ with the difference in solute dipoles $\mu_1^2-\mu_2^2$. According to the predictions of Eq. (1), the free energy difference $\Delta G_{21}$ between states 1 and 2 is directly proportional to $\mu_2^2-\mu_1^2$. If dipole solvation dominates, the scaling of $\Delta G_{21}$ should be linear with $\mu_2^2-\mu_1^2$, and the ratio $G_{21}/(\mu_1^2-\mu_2^2)$ should be identical for the three charge sets.

In the molecular simulation results, the ratio $\Delta G_{21}/(\mu_2^2-\mu_1^2)$ in units of kcal/mol $D^2$ is 0.75 for charge set 1 and 0.76 for charge set 2. The similarity indicates that linear response to a dipole solute is consistent with the solvation energy difference for these two charge sets. The ratio for charge set 3 is larger, 0.89, suggesting that linear response might not be valid for the extreme charges of this charge set.

The results from the continuum calculations differ from the simulation results. First, the ratios are all smaller, reflecting again that the solvation free energies are too small. Second, in this case charge sets 2 and 3 have similar ratios, 0.68 and 0.70, respectively, as should be expected: charge set 3 was obtained from set 2 by a simple scaling of charges. For charge set 1, the ratio is smaller, 0.49, indicating that quadrupole and higher terms are likely to contribute to the solvation. This difference reveals the importance of the molecular charge distribution in determining the solvation energy, even in a continuum calculation.

#### 2. Solvent reorganization energies

The solvent reorganization energies $\lambda$ obtained from simulation are listed in Table V. The results for $\lambda$ predicted by continuum theory are much smaller than the results from molecular simulations, ranging from 38% to 63% of the simulation results. The average absolute error for charge sets 1 and 2 is 1.4 kcal/mol.

The reorganization energy $\lambda$ is predicted theoretically to scale as $(\mu_2-\mu_1)^2$. In the simulations, we find that this scaling is not obeyed. The value of the ratio $\lambda/(\mu_2-\mu_1)^2$ in units of kcal/mol $D^2$ decreases from 2.6 to 1.4 to 1.0 for charge sets 1, 2, and 3. The large ratio for charge set 1 reflects in part the contribution of the quadrupole moment to the reorganization energy. It is also evident, however, that the reorganization energy fails to scale linearly with the square of the transition dipole for solute charge sets 2 and 3, indicating once again that the solvent is not behaving as a dielectric continuum.

In the dielectric continuum calculations, the corresponding ratios are 1.8 for charge set 1, 0.52 for charge set 2, and 0.47 for charge set 3. The quadrupole contribution for charge set 1 is probably responsible for the ratio being larger for

TABLE VII. Reorganization energies in kcal/mol calculated by different methods are compared.

| | Solvent | | | |
|---|---|---|---|---|
| | EQ | FQ/MQ | MQ | TIP4P |
| Charge set 1 | | | | |
| $\lambda$(fluor)[a] | 2.5 | 4.0 | | |
| $\lambda(\Delta E)$[b] | 2.8 | 3.2 | | |
| $\lambda$(abs)[c] | 3.6 | 4.6 | | |
| Charge set 2 | | | | |
| $\lambda$(fluor) | 2.2 | 3.1 | 2.6 | 2.9 |
| $\lambda(\Delta E)$ | 3.0 | 3.2 | 3.2 | 2.8 |
| $\lambda$(abs) | 3.3 | 4.1 | 3.7 | 3.0 |
| Charge set 3 | | | | |
| $\lambda$(fluor) | 11.3 | 19.7 | 11.2 | |
| $\lambda(\Delta E)$ | 24.8 | 25.6 | 27.7 | |
| $\lambda$(abs) | 32.8 | 44.1 | 29.4 | |

[a]From the width $\sigma$ of the fluorescence spectrum, $\lambda=\sigma^2/2k_BT$.
[b]From solvent shifts, $\lambda=(\Delta E_{21}+\Delta E_{12})/2$.
[c]From the width $\sigma$ of the absorption spectrum, $\lambda=\sigma^2/2k_BT$.

charge set 1 than for sets 2 and 3. The ratios for charge sets 2 and 3 are similar to each other, consistent with the predictions from a dielectric continuum model for dipole-only solvation.

#### 3. Fluorescence solvent shifts

The first moment of the solvent shift in a fluorescence spectrum is indicated by $\Delta E_{12}$ in Table V. This quantity tends to be smaller in the molecular simulation results than in the results calculated using a continuum model for the solvent. We compare the results for the polarizable FQ molecular solvent with the results for the most realistic continuum solvent, the polarizable continuum solvent.

For charge set 1, the simulation result is $-0.9$ kcal/mol, while the continuum result is $-0.55$ kcal/mol. These results are very close, essentially within the error bars from simulation.

For the other two charge sets, the simulation results are smaller in magnitude than the results from continuum calculations. For charge set 2, the FQ simulations give an energy of $-4.3$ kcal/mol, compared to $-5.4$ kcal/mol for the continuum solvent. For the 1D→6D transition (charge set 3), FQ simulations give $-6.2$ kcal/mol, but the continuum result is $-12.6$ kcal/mol.

For fluorescence, therefore, the magnitude of the shift in the molecular solvent is smaller than the magnitude of the shift in the continuum solvent. This direction is opposite to the results for absorption, in which the magnitude of the shift in the molecular solvent is larger than the magnitude of the shift in the continuum solvent.

#### 4. Spectral widths and λ

In a solvent obeying linear response, the mean square width $\sigma^2$ of an absorption or fluorescence spectrum is related to the reorganization energy $\lambda$ as

$$\lambda=\sigma^2/2k_BT. \tag{11}$$

In Table VII, we present the reorganization energy $\lambda$ computed by three methods: first, $\lambda(\Delta E)$, the average $(\Delta E_{21}+\Delta E_{12})/2$; second, $\lambda$(abs), from the width of the absorption spectrum according to Eq. (11); and third, $\lambda$(fluor), from the width of the fluorescence spectrum. Results are presented for the four solvents: polarizable FQ, and nonpolarizable FQ/MQ,MQ, and TIP4P.

For each of the solvents and each charge set, a general ordering

$$\lambda(\text{fluor})<\lambda(\Delta E)<\lambda(\text{abs}) \tag{12}$$

is apparent. If the solvent were truly described by linear response, of course, each of these three methods for calculating $\lambda$ would yield an identical result. The inequality indicates that nonlinear behavior is important in describing the response. The ordering $\lambda$(fluor)<$\lambda$(abs) implies that fluctuations in the energy gap between the solute states are larger in the ground state than in the excited state. These two estimates for $\lambda$ tend to bracket the value computed on the basis of $\Delta E$ solvent shifts. For the FQ solvent with charge set 1, for instance, values of $\lambda$ from the spectral widths are 2.5 and 3.6 kcal/mol, bracketing the value of 2.8 kcal/mol from $\Delta E$ measurements. With FQ solvent for charge set 2, the spectral width values 2.2 and 3.3 kcal/mol bracket the $\Delta E$ value $\lambda=3.0$ kcal/mol, etc.

As noted in Sec. IV A, the value of $\lambda(\Delta E)$ is substantially independent of the solvent used in the simulation. Refering to charge set 3, for example, the values for $\lambda(\Delta E)$ are 24.8, 25.6, and 27.7 kcal/mol.

The values for $\lambda$ from the spectral widths, however, show a greater variation with respect to solvent. The polarizable FQ solvent and nonpolarizable MQ solvent tend to produce similar results for $\lambda$, while the nonpolarizable FQ/MQ solvent produces larger values. In charge set 3, for instance, the values of $\lambda$(fluor) from FQ and MQ solvents are 11.3 and 11.2 kcal/mol, while the value from FQ/MQ is 19.7 kcal/mol, roughly 75% larger. For $\lambda$(abs), FQ and MQ give 32.8 and 29.4 kcal/mol, while FQ/MQ gives 44.1 kcal/mol, about 50% larger. This implies that the energy gap fluctuations are larger with the FQ/MQ solvent than with FQ or MQ. Even though the size of the fluctuations depends on the solvent, the similarity of $\lambda(\Delta E)$ serves as a reminder that the average energy gap is roughly the same for all the solvents.

### E. Charge-dependent solute radii in continuum calculations

The differences between the molecular simulations and the continuum calculations might arise from systematic errors in the solute radii used to define the solute cavity in a continuum solvent. In the highly polar ground state, the radii are too large, giving insufficient solvation; in the less polar excited state, the radii are too small, giving too much solvation.

Each model for the ground state of formaldehyde is quite polar, and the default radii for the solute atoms are probably too large. For example, the radius used for the O site in the

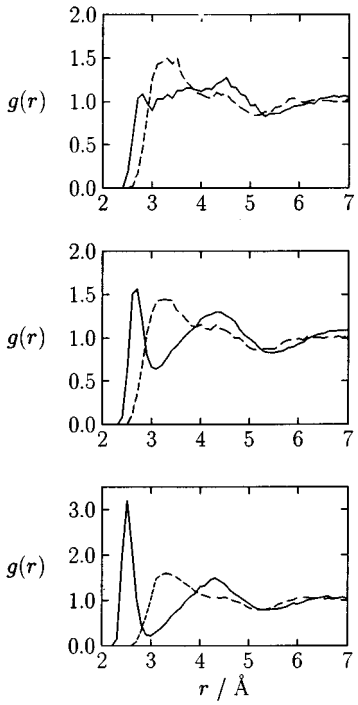


FIG. 1. The radial distribution function $g(r)$, $r$ being the distance between the formaldehyde oxygen and solvent oxygen, is displayed from top to bottom for charge sets 1, 2, and 3. The ground state $g(r)$ is shown as a solid line and the excited state $g(r)$ is a dashed line. The solvent in each case is polarizable FQ water.

continuum theory is 1.60 Å, which in conjunction with the probe radius of 1.53 Å leads to a distance of closest approach of 3.13 Å for solvent molecules with the O site. The center of the probe is generally assumed to represent the center of a solvent molecule, in this case a water molecule, so it is appropriate to compare the distance of 3.13 Å with the first peak in the $g(r)$ between the formaldehyde O and solvent O sites.

Sample $g(r)$ correlations are displayed in Fig. 1. The top, middle, and bottom panels correspond to charge sets 1, 2, and 3, respectively. The ground state $g(r)$ is shown as a solid line; the excited state $g(r)$ is shown as a dashed line. The solvent in each case is polarizable FQ water. The $g(r)$ distributions from the other solvents are similar.

As seen from Fig. 1, the first peak in the ground state OO correlations is located close to 2.5 Å for all three charge sets. This is a much smaller distance than the 3.13 Å implicit in the continuum theory. Thus the continuum solvent does not approach as close to the solute as it should, and the solvation energy is too small.

For the fluorescence lines, the magnitude of the solvent contribution calculated by the dielectric continuum approach is too large. We suggest that this is because the solute radii are too small to represent the apolar excited state solute. Again, the solute and probe radii used by the continuum theory lead to a prediction of a closest distance of 3.13 Å between the solute and solvent O sites. Examination of the OO correlations, the dashed lines in Fig. 1, reveals that the first peak in $g(r)$ is closer to 3.3 Å.

It is interesting to note that for the 1.88 D excited state of charge set 1, the first maximum of the OO peak is also close to 3.3 Å, but the simulation and continuum results for $\Delta E_{12}$ are close in value. The simulation and continuum results might be in better agreement for this transition than for the other two because this transition has substantial quadrupole character.

For all the charge sets, the net effect of the overestimate of the ground state cavity radius and the underestimate of the excited state cavity radius is to reduce the magnitude of $\Delta E_{21}$ and to increase the magnitude of $\Delta E_{12}$. Since $\Delta E_{21}$ is a positive quantity and $\Delta E_{12}$ is a negative quantity, these changes in magnitude cancel when the difference $(\Delta E_{21}-\Delta E_{12})/2=\Delta G_{21}$ is calculated. Therefore, there is a substantial cancellation of errors when $\Delta G_{21}$ is obtained by a continuum calculation. It is also relevant to note that the parameters for the dielectric continuum calculations were optimized by matching calculated solvation energies to experimental measurements for a series of small organic molecules.[24]

In contrast to calculations of $\Delta G_{21}$, calculations of $\lambda$ compound the errors in $\Delta E_{21}$ and $\Delta E_{12}$. Thus $\lambda$ from a continuum calculation tends to be much smaller than the simulation results. A more detailed continuum model with charge-dependent solute radii seems to be necessary for accurate calculations of solvent shifts and solvent reorganization energies.

We have performed a series of continuum calculations employing solute radii that depend on the solute electronic state in an attempt to obtain better agreement between continuum calculations and simulations with explicit molecular solvent. Continuum calculations with charge-dependent solute radii are described in Sec. II C. Several methods were used to define the solute radii. We begin with a description of radii obtained using structural data from $g(r)$. The effective radius defined on the basis of $g(r)$ includes a contribution from the solute and a contribution from the solvent. The probe used to define the solute cavity also represents a solvent radius. To avoid including the solvent radius twice, it is necessary to remove the contribution of the solvent to the radius defined from $g(r)$. We describe two methods of performing this correction, yielding two estimates for effective ground and excited state radii: $R_{\mathrm{eff}}^{q}$, based on $g(r)$ for pure solvent, and $R_{\mathrm{eff}}^{\mathrm{fit}}$, based on a single-parameter fit to the molecular simulation data. We also describe a third method for arriving at an effective radius, suggested by Rick and Berne.[57] It is defined by the distance at the first nonzero value of $g(r)$ and termed here $R_{\mathrm{eff}}^{\mathrm{RB}}$. This definition of an effective radius is similar to definitions used in studies of pore size distributions and cavity radius distributions.[72,73]

#### 1. $R_{\mathrm{eff}}^{g}$, charge-dependent solute radii from $g(r)$

For a spherical ion in an atomic solvent, an effective solute radius can be defined directly from the solute–solvent radial distribution function $g(r)$ as[74]

TABLE VIII. Effective radii[a] $R_{\mathrm{eff}}^{g}$,[b] $R_{\mathrm{eff}}^{\mathrm{fit}}$,[c] and $R_{\mathrm{eff}}^{\mathrm{RB}}$.[d]

| | Charge set 1 | | | Charge set 2 | | | Charge set 3 | | |
|---|---|---|---|---|---|---|---|---|---|
| | $R_{\mathrm{eff}}^{q}$ | $R_{\mathrm{eff}}^{\mathrm{fit}}$ | $R_{\mathrm{eff}}^{\mathrm{RB}}$ | $R_{\mathrm{eff}}^{q}$ | $R_{\mathrm{eff}}^{\mathrm{fit}}$ | $R_{\mathrm{eff}}^{\mathrm{RB}}$ | $R_{\mathrm{eff}}^{g}$ | $R_{\mathrm{eff}}^{\mathrm{fit}}$ | $R_{\mathrm{eff}}^{\mathrm{RB}}$ |
| Ground state | | | | | | | | | |
| O | 1.74 | 1.49 | 1.5 | 1.66 | 1.41 | 1.4 | 1.41 | 1.16 | 1.4 |
| C | 1.96 | 1.71 | 2.1 | 1.94 | 1.69 | 2.0 | 1.80 | 1.55 | 2.1 |
| H | 1.73 | 1.48 | 1.7 | 1.70 | 1.45 | 1.8 | 1.59 | 1.34 | 1.8 |
| Excited state | | | | | | | | | |
| O | 1.83 | 1.58 | 1.7 | 1.78 | 1.53 | 1.6 | 1.82 | 1.57 | 1.7 |
| C | 1.98 | 1.73 | 1.8 | 1.95 | 1.70 | 2.0 | 1.98 | 1.73 | 2.1 |
| H | 1.74 | 1.49 | 1.7 | 1.71 | 1.46 | 1.7 | 1.74 | 1.46 | 1.7 |

[a]All values are in Å. The default radii used by PBF are 1.6, 1.95, and 1.15 Å for O, C, and H, respectively.
[b]$R_{\mathrm{eff}}^{g}=[\int_0^\infty dr\, g(r)/r^2]^{-1}-0.75$.
[c]$R_{\mathrm{eff}}^{\mathrm{fit}}=[\int_0^\infty dr\, g(r)/r^2]^{-1}-1$.
[d]$R_{\mathrm{eff}}^{\mathrm{RB}}$ is the position of the first nonzero value of $g(r)$ between a solute site and either the H or O site of solvent water.

$$R_{\mathrm{eff}}^{g}=\left[\int dr\; g(r)/r^2\right]^{-1}. \tag{13}$$

The superscript $g$ serves as a reminder that the definition is based on $g(r)$. For a trivial solute–solvent correlation $g(r)$ that is 0 inside a hard core radius $R$ and 1 outside the hard core, $R_{\mathrm{eff}}^{g}=R$. This formula provides a method to identify a similar structural radius for a general $g(r)$, but is ultimately based on considerations of solvent fluctuations around an ionic solute.[74]

We have used Eq. (13) to define formaldehyde solute radii that depend on the electronic state. For each solute site, O, C, and H, the correlation $g(r)$ between the solute site and the O site of polarizable FQ solvent was obtained from simulation data. The raw values provided by Eq. (13) include a contribution from the solvent radius. In continuum calculations, however, the solvent radius enters as the radius of the probe that is used to define the molecular surface. Thus since we desire to continue to use a probe radius of 1.4 Å, the raw values of $R_{\mathrm{eff}}^{g}$ must be reduced to account for the contribution of the solvent molecules.

Subtracting the entire probe radius of 1.4 Å gives radii that are much too small. We inspect the value of $R_{\mathrm{eff}}^{g}$ for water in water to guide in the subtraction. In pure SPC water, $g_{\mathrm{OO}}(r)$ gives $R_{\mathrm{eff}}^{g}=2.24$ Å. Values obtained for other water models, like TIP4P-FQ and TIP4P, are not significantly different.

If the $H_2O$ molecule is regarded as a solute, we are to choose a correction $\Delta R$ such that the corrected solute radius $R_{\mathrm{eff}}^{g}-\Delta R$ is equal to the default radius of 1.6 Å used by the PBF program. This procedure yields $\Delta R=0.64$ Å. Alternatively, it is possible to think of $H_2O$ instead as a solvent molecule. In this case, the subtraction $R_{\mathrm{eff}}^{g}-\Delta R$ is associated with the probe radius itself, 1.4 Å, yielding $\Delta R=0.84$ Å.

The difference between these two approaches, 0.64 vs 0.84 Å, simply reflects the inequality of different O sites in the default PBF parameterization: solute O sites have a radius that is 0.2 Å larger than solvent O sites. As a compromise, we use $\Delta R=0.75$, giving the corrected radii that are listed under the column $R_{\mathrm{eff}}^{g}$ in Table VIII.

Except for the highly polar ground state of charge set 3, the O radii presented in Table VIII are larger than the PBF default value, 1.6 Å. The C radii are all close to the default value of 1.95 Å, and the H radii, roughly 1.7 Å, are much larger than the default value of 1.15 Å. As seen in Table IX, these radii produce solvation energies that are similar to the results using the default radii.

### 2. $R_{\mathrm{eff}}^{\mathrm{fit}}$, solute radii from a single-parameter fit

In an attempt to improve the agreement with the simulation data, we performed a single-parameter optimization of

TABLE IX. Solvation energies from molecular simulation and from continuum calculations with charge-dependent radii.[a]

| | FQ simulation | Continuum calculation | | | |
|---|---|---|---|---|---|
| | | Default radii | $R_{\mathrm{eff}}^{g}$ | $R_{\mathrm{eff}}^{\mathrm{fit}}$ | $R_{\mathrm{eff}}^{\mathrm{RB}}$ |
| Charge set 1 | | | | | |
| $E_{21}$ | 6.4 | 4.3 | 4.1 | 6.3 | 5.2 |
| $E_{12}$ | −0.9 | −0.6 | −1.1 | −1.1 | −1.4 |
| $G_{21}$ | 3.7 | 2.4 | 2.6 | 3.7 | 3.3 |
| λ | 2.8 | 1.9 | 1.5 | 2.6 | 1.9 |
| Charge set 2 | | | | | |
| $E_{21}$ | 10.2 | 7.6 | 7.0 | 10.1 | 8.7 |
| $E_{12}$ | −4.3 | −5.4 | −4.6 | −6.7 | −5.7 |
| $G_{21}$ | 7.3 | 6.5 | 5.8 | 8.4 | 7.2 |
| λ | 3.0 | 1.1 | 1.2 | 1.7 | 1.5 |
| Charge set 3 | | | | | |
| $E_{21}$ | 55.7 | 36.1 | 40.4 | 60.6 | 35.3 |
| $E_{12}$ | −6.2 | −12.6 | −12.6 | −18.8 | −11.1 |
| $G_{21}$ | 31.0 | 24.3 | 26.5 | 39.7 | 23.2 |
| λ | 24.8 | 11.8 | 13.9 | 20.9 | 12.1 |

[a]All energies are in kcal/mol. The solvent in the simulations is polarizable TIP4P-FQ. The continuum solvent is polarizable with $\epsilon_0=80.37$ and $\epsilon_\infty=1.592$.

the effective radii $R_{\rm eff}^{g}$ defined by $g(r)$. The raw value of $R_{\rm eff}^{g}$ contains a contribution corresponding to an effective solvent radius $\Delta R$ that must be subtracted when a probe radius is used to define the molecular surface. In the previous section we estimated $\Delta R$ from $g(r)$ for pure solvent; in this section we perform a one-parameter fit to determine $\Delta R$.

The single parameter was optimized by fitting the free energy difference $G_{21}$ to the values for $G_{21}$ from simulations with TIP4P-FQ solvent for charge set 1 ($G_{21}=3.7$ kcal/mol), the most realistic of the three charge sets. We found that $\Delta R=1$ Å gave good agreement, with changes of 0.025 Å noticeably worse. The solute radii obtained by this fit are

$$R_{\rm eff}^{\rm fit}=\left[\int dr\ g(r)/r^2\right]^{-1}-1\ \ \text{Å}. \tag{14}$$

Other, more elaborate schemes might provide better fits to the data. Our intention, however, is to understand at a qualitative level whether a fit at a single point is sufficient to describe the totality of data.

The radii $R_{\rm eff}^{\rm fit}$ for O and C are generally smaller than the radii used by default in PBF. The O site in the charge set 1 ground state, for instance, is 1.49 Å, versus a default value of 1.6 Å. The contraction in the radii in the increasingly polar ground states of charge sets 1, 2, and 3 is also evident. The O site radius decreases from 1.49 to 1.16 Å in this series. The effective radii $R_{\rm eff}^{\rm fit}$ for the H sites in the solute are somewhat larger than the default radius of 1.15 Å used by PBF. This compensates to some extent for the smaller radius obtained for C.

Solvation energies calculated in a continuum solvent on the basis of the radii $R_{\rm eff}^{\rm fit}$ are presented in Table IX. The agreement with molecular simulation for charge set 1 is very good, not just for $G_{21}$ (which served as the basis of the parameterization), but for $\lambda$ as well. This indicates clearly that with proper parameterization, it is indeed possible to reproduce molecular simulation solvation energies using a continuum solvent instead.

For the remaining two charge sets, however, the agreement is not as good as for charge set 1. The values of $G_{21}$ are too large, and the values of $\lambda$ are too small. To obtain better agreement, it would be necessary to reparameterize the fit value $\Delta R$ for charge sets 2 and 3.

### 3. $R_{\rm eff}^{RB}$, radii based on the rise of $g(r)$

Previous continuum studies using charge-dependent radii agreed with molecular simulations when the effective solute radii were defined from simulation $g(r)$ data as the distance where $g(r)$ between a solute site and either O or H of solvent water first became nonzero.[57] Using simulation data from formaldehyde in FQ water, we determined these distances, termed $R_{\rm eff}^{\rm RB}$ and presented in Table VIII. Distances from simulations employing TIP4P-MQ or TIP4P solvent are within 0.1 Å of the distances obtained with TIP4P-FQ water.

Continuum calculations of solvation energies using $R_{\rm eff}^{\rm RB}$ are similar to energies obtained using the default radii. The agreement with molecular simulation is not as good as it was with $R_{\rm eff}^{\rm fit}$, but is better than $R_{\rm eff}^{g}$.

## V. CONCLUSION

We have demonstrated that a molecular model for formaldehyde, with charges derived from *ab initio* electrostatic potential fitting and standard Lennard-Jones parameters, combined with a molecular model for polarizable water, produces a solvent shift in an absorption line in very good agreement with experimental results for acetone, a molecule expected to have a solvent shift similar to that of formaldehyde.

We find that it is important to use a method like electrostatic potential fitting (ESP) to obtain the solute ground and excited state charges. The *ab initio* electronic structure used as the basis for the fitting should include the additional polarization of a solvated molecule that enhances the charges from gas phase values. Other methods, in particular natural population analysis (NPA) and similar techniques, can produce charges that are far too large. These unrealistically large charges exaggerate the solvent interactions and predict excessively large solvation energies.

Polarizable and nonpolarizable molecular solvents produce similar results for equilibrium properties like free energy differences. In disagreement with theoretical linear-response predictions, however, the nonequilibrium solvation energies from polarizable and nonpolarizable solvents also agree quite closely. This indicates that scaling formulas commonly used to relate solvent reorganization energies in the two classes of solvent might be incorrect.

We also performed detailed calculations using a continuum solvent surrounding explicit molecular solutes. The solutes in these calculations had the same charge distributions as in the molecular simulations. The solute cavities were defined using standard atomic radii parameterized for typical molecular solutes. We found that the solvation energy from the continuum solvent was too small for the highly polar ground state solutes and was too large for the relatively non-polar excited state solutes. Using a single set of radii for ground and excited states contributes to this disagreement. A continuum model that accounts for molecular size effects,[48] or one with more parameters, such as solute radii that depend on solute atom types and charges,[75] can provide better agreement with experimental and molecular simulation results. The many-parameter approach can be unwieldy, however, as atom types become highly differentiated, each with its own parameters that must be fit to particular thermodynamic states.

An entirely different route to calculating solvation energies without the need for molecular simulations is provided by integral equation methods, which provide a microscopic picture of solvation phenomena.[76] The reference interaction site model (RISM) is an integral equation theory based on two-point pairwise correlations between molecular sites and an approximate closure relation.[77] The RISM equation is computationally tractable because its iterative solution reduces to a series of one-dimensional transforms; it has been used to describe nonpolar solvents,[78,79] conformational equilibria,[80] hydrophobic hydration,[81] polar solvation,[82] and solvation in polarizable media.[83,84] A recognized shortcom-

ing of RISM methods, however, is the difficulty in treating large molecules' solvent inaccessible sites using two-point correlation functions.[85,86] Recent attempts to develop efficient algorithms for solving fully three-dimensional integral equations have the promise of overcoming this difficulty,[87–90] and might eventually provide a computationally feasible alternative to dielectric continuum methods for calculating solvation energies and structures.

## ACKNOWLEDGMENTS

This work was supported by a grant from the National Science Foundation (NSF-CHE-91-22506). Portions of the computational work were performed on the Thinking Machines CM5 of the NIH Research Resource Center of the Columbia Center for Biomolecular Simulations. We thank Bryan Marten and Daniel T. Mainz for assistance with the electronic structure calculations using PS-GVB.

## APPENDIX: FLUCTUATING CHARGES AND QUANTUM MECHANICS

The contribution of the electronic polarization modes to the solvation energy is inherently quantum mechanical, yet the FQ model represents these modes as classical degrees of freedom. Nevertheless, the solvation energies obtained using the polarizable FQ model are consistent with those that would be obtained with an explicit quantum treatment. We support this claim with a calculation for a simplified model system comprising a two level system (TLS), representing two electronic states of a solute molecule, and a single harmonic oscillator, representing an electronic polarization mode. This model is based closely on similar spin-Boson models for charge transfer systems.[15–17] For simplicity, the model does not include an analog of the classical nuclear degrees of freedom of a molecular solvent. Including slow nuclear modes would not change the analysis below because such modes are fixed during an electronic transition according to a Condon approximation.

The Hamiltonian for this simple model system is

$$H=\begin{pmatrix} \epsilon_0-q\mu_0 & -K \\ -K & \epsilon_1-q\mu_1 \end{pmatrix}+\frac{1}{2\alpha}\,q^2+\frac{1}{2}\,\alpha\omega^2p^2. \quad \text{(A1)}$$

The states of the TLS are labeled ''1'' and ''2'' with energies $\epsilon_1$ and $\epsilon_2$. The states are coupled by the term $K$. The oscillator coordinate $q$, with conjugate momentum $p$, has a frequency $\omega$, polarizability $\alpha$, and mass $m$. The two level system and the oscillator are coupled linearly with the term $-q\mu_i$, $i=1$ or 2 depending on the state of the TLS.

Neglecting terms of order $K$, which we assume to be small relative to other energies, we proceed with a quantum mechanical calculation of the energy gap between the two electronic states of the system with diabats

$$H_i=\epsilon_i-q\mu_i+\frac{1}{2\alpha}\,q^2+\frac{1}{2}\,\alpha\omega^2p^2. \quad \text{(A2)}$$

A routine calculation, assuming that the oscillator remains in its ground vibrational state during the transition, yields

$$E_i=\tfrac{1}{2}\hbar\omega+\epsilon_i-\tfrac{1}{2}\alpha\mu_i^2. \quad \text{(A3)}$$

for the energies of the ground ($i=1$) and excited ($i=2$) electronic states. The energy gap $\Delta E_{21}$ is $E_2-E_1$, or

$$\Delta E_{21}=\epsilon_2-\epsilon_1-\tfrac{1}{2}\alpha(\mu_2^2-\mu_1^2). \quad \text{(A4)}$$

The treatment of the electronic polarization modes in the simulations corresponds to a classical treatment of the coordinate $q$, with two special provisions. First, the coordinate $q$ is kept at a low temperature $T_Q$. (In the FQ simulations, $T_Q$ was approximately 1 K, while the temperature of the nuclear modes was 298 K.) Second, the coordinate is allowed to relax before an energy gap is calculated. Thus a calculation of the energy gap $\Delta E_{21}$ corresponding to our treatment of electronic polarization in FQ water yields

$$\Delta E_{21}=\langle H_2\rangle_2-\langle H_1\rangle_1 \quad \text{(A5)}$$

$$=k_BT_Q+\epsilon_2-\tfrac{1}{2}\alpha\mu_2^2 \quad \text{(A6)}$$

$$-(k_BT_Q+\epsilon_1-\tfrac{1}{2}\alpha\mu_1^2) \quad \text{(A7)}$$

$$=\epsilon_2-\epsilon_1-\tfrac{1}{2}\alpha(\mu_2^2-\mu_1^2), \quad \text{(A8)}$$

identical to the quantum mechanical result. The thermal averages in the above equations are defined as

$$\langle\cdots\rangle_i=\frac{\mathrm{Tr}\; e^{-\beta H_i}(\cdots)}{\mathrm{Tr}\; e^{-\beta H_i}} \quad \text{(A9)}$$

for $i=1$ or 2.

Our results with the FQ method correspond to quantum mechanical energy differences because the polarization modes do not obey a Condon approximation during an electronic transition of the solute. Under a Condon approximation, the mode $q$ would be fixed during an electronic transition. The energy gap $\Delta E_{21}$ for absorption from state 1 to state 2 would then be given by the thermodynamic average

$$\Delta E_{21}=\langle H_2-H_1\rangle_1 \quad \text{(A10)}$$

$$=\epsilon_2-\epsilon_1-\alpha\mu_1(\mu_2-\mu_1). \quad \text{(A11)}$$

Comparison of Eq. (A10) to Eq. (A3) indicates that the Condon approximation for the polarization modes produces an energy that is incorrect.

[1] R. A. Marcus, J. Am. Chem. Soc. **24**, 966 (1956).
[2] R. A. Marcus, J. Am. Chem. Soc. **24**, 979 (1956).
[3] R. A. Marcus and N. Sutin, Biochim. Biophys. Acta **811**, 265 (1985).
[4] R. A. Marcus, Rev. Mod. Phys. **65**, 599 (1993).
[5] P. G. Wolynes, J. Chem. Phys. **87**, 6559 (1987).
[6] M. J. Gillan, J. Phys. C **20**, 3621 (1987).
[7] G. A. Voth, D. Chandler, and W. H. Miller, J. Chem. Phys. **91**, 7749 (1989).
[8] J. S. Bader, R. A. Kuharski, and D. Chandler, J. Chem. Phys. **93**, 230 (1990).
[9] A. Warshel and J.-K. Hwang, J. Chem. Phys. **84**, 4938 (1986).
[10] A. Warshel, Z. T. Chu, and W. W. Parson, Science **246**, 112 (1989).
[11] A. Warshel and W. W. Parson, Annu. Rev. Phys. Chem. **42**, 279 (1991).
[12] J. Lobaugh and G. A. Voth, J. Chem. Phys. **100**, 3039 (1994).
[13] J. B. Straus, A. Calhoun, and G. A. Voth, J. Chem. Phys. **102**, 529 (1995).
[14] J. Lobaugh and G. A. Voth, J. Chem. Phys. **104**, 2056 (1996).
[15] J. N. Gehlen, D. Chandler, H. J. Kim, and J. T. Hynes, J. Phys. Chem. **96**, 1748 (1992).
[16] J. N. Gehlen and D. Chandler, J. Chem. Phys. **97**, 4958 (1992).

[17] X. Song and R. A. Marcus, J. Chem. Phys. **99**, 7768 (1993).
[18] J. J. Zhu and R. I. Cukier, J. Chem. Phys. **102**, 8398 (1995).
[19] J. S. Bader and B. J. Berne, J. Chem. Phys. **104**, 1293 (1996).
[20] J. Warwicker and H. C. Watson, J. Mol. Biol. **157**, 671 (1982).
[21] M. K. Gilson, K. A. Sharp, and B. Honig, J. Comput. Chem. **9**, 327 (1988).
[22] A. Nicholls and B. Honig, J. Comput. Chem. **12**, 435 (1991).
[23] B. Honig and A. Nicholls, Science **268**, 1144 (1995).
[24] D. J. Tannor, B. Marten, and R. Murphy, J. Am. Chem. Soc. **116**, 11875 (1994).
[25] V. Luzhkov and A. Warshel, J. Am. Chem. Soc. **113**, 4491 (1991).
[26] R. G. Alden, W. W. Parson, Z. T. Chu, and A. Warshel, J. Am. Chem. Soc. **117**, 12284 (1995).
[27] S. W. Rick, S. J. Stuart, and B. J. Berne, J. Chem. Phys. **101**, 6141 (1994).
[28] W. L. Jorgensen, J. Chandrasekhar, and J. D. Madura, J. Chem. Phys. **79**, 926 (1983).
[29] H. H. Jaffe and M. Orchin, *Theory and Applications of U.V. Spectroscopy* (Wiley, New York, 1962).
[30] R. Cimiraglia, S. Miertus, and J. Tomasi, Chem. Phys. Lett. **80**, 286 (1981).
[31] P. R. Taylor, J. Am. Chem. Soc. **104**, 5248 (1982).
[32] R. Bonaccorsi, R. Cimiraglia, and J. Tomasi, Chem. Phys. Lett. **99**, 77 (1983).
[33] J. T. Blair, K. Krogh-Jespersen, and R. M. Levy, J. Am. Chem. Soc. **111**, 6948 (1989).
[34] J. T. Blair, R. M. Levy, and K. Krogh-Jespersen, Chem. Phys. Lett. **166**, 429 (1990).
[35] M. A. Aguilar, F. J. Olivares del Valle, and J. Tomasi, J. Chem. Phys. **98**, 7375 (1993).
[36] Y. Dimitrova and S. Peyerimhoff, J. Phys. Chem. **97**, 12731 (1993).
[37] S. Ten-no, F. Hirata, and S. Kato, J. Chem. Phys. **100**, 7443 (1994).
[38] K. V. Mikkelsen, A. Cesar, H. Ågren, and H. J. A. Jensen, J. Chem. Phys. **103**, 9010 (1995).
[39] M. L. Sánchez, M. A. Aquilar, and F. J. Olivares del Valle, J. Phys. Chem. **99**, 15758 (1995).
[40] H. Fukunaga and K. Morokuma, J. Phys. Chem. **97**, 59 (1993).
[41] R. M. Levy, D. B. Kitchen, J. T. Blair, and K. Krogh-Jespersen, J. Phys. Chem. **94**, 4470 (1990).
[42] S. E. Debolt and P. A. Kollman, J. Am. Chem. Soc. **112**, 7515 (1990).
[43] A. M. Kuznetsov, J. Phys. Chem. **96**, 3337 (1992).
[44] R. A. Marcus, J. Phys. Chem. **96**, 1753 (1992).
[45] M. Marchi, J. N. Gehlen, D. Chandler, and M. Newton, J. Am. Chem. Soc. **115**, 4178 (1993).
[46] R. M. Levy, M. Belhadj, and D. B. Kitchen, J. Chem. Phys. **95**, 3627 (1991).
[47] R. M. Levy, J. D. Westbrook, D. B. Kitchen, and K. Krogh-Jespersen, J. Phys. Chem. **95**, 6756 (1991).
[48] G. J. Tawa and L. R. Pratt, in *Structure and Reactivity in Aqueous Solution: Characterization of Chemical and Biological Systems*, edited by C. J. Cramer and D. G. Truhlar (American Chemical Society, Washington, D.C., 1994), Chap. 5, pp. 60–70.
[49] M. P. Allen and D. J. Tildesley, *Computer Simulation of Liquids* (Oxford University Press, New York, 1987).
[50] K. Sharp, A. Jean-Charles, and B. Honig, J. Phys. Chem. **96**, 3822 (1992).
[51] S. W. Rick and B. J. Berne, J. Am. Chem. Soc. **118**, 672 (1996).
[52] S. J. Stuart and B. J. Berne, J. Phys. Chem. **100**, 11934 (1996).
[53] C. J. F. Bottcher, *Theory of Electric Polarization* (Elsevier Scientific, New York, 1978).
[54] D. V. Matyushov and R. Schmid, J. Phys. Chem. **98**, 5152 (1994).
[55] D. V. Matyushov and R. Schmid, Mol. Phys. **84**, 533 (1995).
[56] C. Cortis and R. A. Friesner, J. Comput. Chem. (in press).
[57] S. W. Rick and B. J. Berne, J. Am. Chem. Soc. **116**, 3949 (1994).
[58] M. F. Herman and B. J. Berne, Chem. Phys. Lett. **77**, 163 (1981).
[59] K. S. Schweizer and D. Chandler, J. Chem. Phys. **76**, 2296 (1982).
[60] K. Kondo and T. Oka, J. Phys. Soc. Jpn. **15**, 307 (1960).
[61] A. D. Buckingham, D. A. Ramsey, and J. Tyrell, Can. J. Phys. **48**, 1242 (1970).
[62] D. E. Freeman and W. Klemperer, J. Chem. Phys. **45**, 52 (1966).
[63] V. T. Jones and J. B. Coon, J. Mol. Spectrosc. **31**, 137 (1969).
[64] M. J. Frisch, G. W. Trucks, M. Head-Gordon, P. M. W. Gill, M. W. Wong, J. B. Foresman, B. G. Johnson, H. B. Schlegel, M. A. Robb, E. S. Replogle, R. Gomperts, J. L. Andres, K. Raghavachari, J. S. Binkley, C. Gonzalez, R. L. Martin, D. J. Fox, D. J. Defrees, J. Baker, J. J. P. Stewart, and J. A. Pople, GAUSSIAN 92, Revision C.4, Gaussian, Inc., Pittsburgh, 1992.
[65] Murco N. Ringnalda, Jean-Marc Langlois, Burnham H. Greeley, Robert B. Murphy, Thomas V. Russo, Christian Cortis, Richard P. Muller, Bryan Marten, Robert E. Donnelly, Jr., Daniel T. Mainz, Julie R. Wright, W. Thomas Pollard, Yixiang Cao, Youngdo Won, Gregory H. Miller, William A. Goddard III, and Richard A. Friesner, PS-GVB v2.02, Schrodinger, Inc., 1994.
[66] F. M. Richards, Annu. Rev. Biophys. Bioeng. **6**, 151 (1977).
[67] A. E. Reed, R. B. Weinstock, and F. Weinhold, J. Chem. Phys. **83**, 735 (1985).
[68] B. Fabricant, D. Krieger, and J. S. Muenter, J. Chem. Phys. **67**, 1576 (1977).
[69] GAUSSIAN 92 has two options for electrostatic charge fitting, chelp and chelpg. We found that chelpg produced reasonable results, but that chelp gave very unrealistic charges. Furthermore, when the dipole moment from the charges was constrained to match the dipole moment from the electronic structure calculation, an error in the program produced erroneous charges and a net dipole of 13 D.
[70] E. R. Davidson, Chem. Phys. Lett. **21**, 565 (1973).
[71] H. C. Andersen, J. Comput. Phys. **52**, 24 (1983).
[72] K. Gotoh, M. Nakagawa, M. Furuuchi, and A. Yoshigi, J. Chem. Phys. **85**, 3078 (1986).
[73] H. Tanaka, J. Chem. Phys. **86**, 1512 (1987).
[74] L. R. Pratt. (personal communication).
[75] C. J. Cramer and D. G. Truhlar, J. Am. Chem. Soc. **113**, 8305 (1991).
[76] J. P. Hansen and I. R. McDonald, *Theory of Simple Liquids* (Academic, London, 1986).
[77] D. Chandler and H. C. Andersen, J. Chem. Phys. **57**, 1930 (1972).
[78] L. J. Lowden and D. Chandler, J. Chem. Phys. **59**, 6587 (1973).
[79] L. J. Lowden and D. Chandler, J. Chem. Phys. **61**, 5228 (1974).
[80] L. R. Pratt and D. Chandler, J. Chem. Phys. **66**, 147 (1977).
[81] L. R. Pratt and D. Chandler, J. Chem. Phys. **67**, 3683 (1977).
[82] F. Hirata and P. J. Rossky, J. Chem. Phys. **83**, 329 (1981).
[83] B.-C. Perng, M. D. Newton, F. O. Raineri, and H. L. Friedman, J. Chem. Phys. **104**, 7153 (1996).
[84] B.-C. Perng, M. D. Newton, F. O. Raineri, and H. L. Friedman, J. Chem. Phy. **104**, 7177 (1996).
[85] B. M. Pettitt and M. Karplus, Chem. Phys. Lett. **136**, 383 (1987).
[86] D. Laria, D. Wu, and D. Chandler, J. Chem. Phys. **95**, 444 (1991).
[87] D. Beglov and B. Roux, J. Chem. Phys. **103**, 360 (1995).
[88] D. Beglov and B. Roux, J. Chem. Phys. **104**, 8678 (1996).
[89] M. Ikeguchi and J. Doi, J. Chem. Phys. **103**, 5011 (1995).
[90] C. Cortis, P. J. Rossky, and R. A. Friesner (manuscript in preparation).